

Onset of sliding friction in incommensurate systems

L. Consoli, H. J. F. Knops, and A. Fasolino

Institute for Theoretical Physics, University of Nijmegen, Toernooiveld 1, 6525 ED Nijmegen, The Netherlands
(December 2, 2024)

We study the dynamics of an incommensurate chain sliding on a periodic lattice, modeled by the Frenkel Kontorova hamiltonian with initial kinetic energy, without damping and driving terms. We show that the onset of friction at all velocities is due to a novel kind of dissipative parametric resonances, involving several resonant phonons which are driven by the (dissipationless) coupling of the center of mass motion to the phonons with wavevector related to the modulating potential. We establish quantitative estimates for their existence in finite systems and point out the analogy with the induction phenomenon in Fermi-Ulam-Pasta lattices.

PACS numbers: 05.45.-a, 45.05.+x, 46.55.+d, 46.40.Ff

The possibility of measuring friction at the atomic level provided by the Lateral Force Microscopes [1] and Quartz Crystal Microbalance [2] has stimulated intense research on this topic [3]. Most studies are carried out for one-dimensional models of non-linear lattices [4–11] and in particular for the Frenkel-Kontorova (FK) model [12], where the surface layer is modeled by a harmonic chain and the substrate is replaced by a rigid periodic modulation potential. The majority [5–11] examines the steady state of the dynamic FK model in presence of driving forces in dissipative cases which can better describe experimental conditions. The drawback of this approach is that dissipation due to undescribed degrees of freedom is brought in phenomenologically via a friction coefficient and that transient phenomena are not examined. Here we show that letting the system evolve without external and damping forces allows to identify in detail the microscopic mechanisms for energy dissipation during the sliding of a body onto a crystalline surface.

We study the dynamics of an undriven, undamped incommensurable FK chain as a function of the initial center of mass (CM) velocity and of the coupling to the substrate potential. We focus on coupling values below the static Aubry transition [13] where the CM motion is not locked. For this case, Shinjo and Hirano [4] have predicted a *superlubric* regime where the chain would slide indefinitely without dynamic friction but with a recurrent exchange of kinetic energy between CM and internal vibrations. We will show that their phase diagram is oversimplified since the inherent non-linear coupling of the CM to the phonons leads to an irreversible decay of the CM velocity, albeit with very long time scales in some windows. The dissipative mechanism is driven by the coupling of the CM to the mode with modulation wavevector q or its harmonics, ω_{nq} , and consists in a novel kind of parametric resonances. This leads to much wider windows of instabilities than those deriving from the standard Mathieu equation [14]. The importance of (super)harmonic resonances at ω_{nq} has been pointed out before [5,7,9], together with the suggestion [9] that they

could be absent in finite systems due to the discreteness of the phonon spectrum. However, it has not been realized that they act as a *driving* term for the onset of dissipation via subsequent complex parametric excitations which we shall describe, establishing quantitative estimates for their existence in finite systems. A related mechanism has recently been identified in the resonant energy transfer in the induction phenomenon in Fermi-Ulam-Pasta lattices [15].

We start with the FK hamiltonian

$$\mathcal{H} = \sum_{n=1}^N \left[\frac{p_n^2}{2} + \frac{1}{2} (u_{n+1} - u_n - l)^2 + \frac{\lambda}{2\pi} \sin\left(\frac{2\pi u_n}{m}\right) \right] \quad (1)$$

where u_n are the lattice positions and l is the equilibrium spacing of the chain for $\lambda = 0$, λ being the strength of the coupling scaled to the elastic spring constant. We assume an incommensurable ratio of l to the period m of the periodic potential, namely $m = 1$, $l = (1 + \sqrt{5})/2$. We consider chains of N atoms with N large and with periodic boundary conditions $u_{N+1} = Nl + u_1$. Therefore, in the numerical implementation, we have to choose commensurate approximations for l so that $l \times N = M \times 1$ with N and M integer, i.e. we express l as ratio of consecutive Fibonacci numbers. The ground state of this model displays the so called Aubry transition [13] from a modulated to a pinned configuration above a critical value $\lambda_c = 0.14$. Here we just note that in the limit of weak coupling ($\lambda \ll \lambda_c$), deviations from equidistant spacing l in the ground state are modulated with the substrate modulation wavevector $q = 2\pi l/m$ [16] as due to the frozen-in phonon ω_q . Higher harmonics nq have amplitudes which scale with λ^n .

We define the CM position and velocity as $Q = \frac{1}{N} \sum_n u_n$, $P = \frac{1}{N} \sum_n p_n$. By writing $u_n = nl + x_n + Q$, the equations of motion for the deviations from a rigid displacement x_n read

$$\ddot{x}_n = x_{n+1} + x_{n-1} - 2x_n + \lambda \cos(qn + 2\pi x_n + 2\pi Q) \quad (2)$$

We integrate by a Runge Kutta algorithm the N equations (2) with initial momenta $p_n = P_0$ and $x_n(t=0)$ corresponding to the ground state. For a given velocity P , particles pass over maxima of the potential with frequency $\Omega = 2\pi P$, the so-called washboard frequency [7,9]. In Fig. 1 we show the time evolution of the CM momentum for $\lambda \sim \lambda_c/3$ and several values of P_0 . According to the phase diagram of Ref. [4] a superlubric behavior should be observed for this value of λ and $P_0 \geq 0.1$. We find instead a non trivial time evolution with oscillations of varying period and amplitude and, more remarkably, a very fast decay of the CM velocity for $P_0 \sim \omega_q/(2\pi)$ despite the absence of a damping term in Eq. (2). A similar, but less pronounced, decay is observed for $nP_0 \sim \omega_{nq}/(2\pi)$. In the study of the driven underdamped FK [7] it is shown that, at these superharmonic resonances, the differential mobility is extremely low. Here, we work out an analytical description in terms of the phonon spectrum which explains this complex time evolution and identifies the dissipative mechanism which is triggered by these resonances. In the limit of weak coupling λ it is convenient to go from real to reciprocal space by defining Fourier transformed coordinates:

$$x_k = \frac{1}{N} \sum_n e^{-ikn} x_n \quad ; \quad x_n = \sum_k e^{ikn} x_k \quad (3)$$

where $k = 2\pi n/N$ and the normalization is chosen to remove the explicit N -dependence in the equations of motion which become:

$$\ddot{x}_k = -\omega_k^2 x_k + \frac{\lambda}{2N} \sum_n e^{-ikn} [e^{iqn} e^{i2\pi Q} e^{i2\pi x_n} + c.c.] \quad (4a)$$

$$\ddot{Q} = \frac{\lambda}{2N} \sum_n [e^{i2\pi Q} e^{iqn} e^{i2\pi x_n} + c.c.] \quad (4b)$$

with $\omega_k = 2|\sin(k/2)|$. We expand Eq. (4a) in x_n as:

$$\ddot{x}_k = -\omega_k^2 x_k + \frac{\lambda}{2} \sum_{m=0}^{\infty} \frac{(i2\pi)^m}{m!} \sum_{k_1 \dots k_m} [e^{i2\pi Q} x_{k_1} \dots x_{k_m} \delta_{k_1 + \dots + k_m, -q+k} + (-1)^m e^{-i2\pi Q} x_{k_1} \dots x_{k_m} \delta_{k_1 + \dots + k_m, q+k}] \quad (5)$$

Since in the ground state the only modes present in order λ are $x_q = x_{-q} = \lambda/2\omega_q^2$ the CM is coupled only to these modes up to second order in λ :

$$\ddot{Q} = i\lambda\pi (e^{i2\pi Q} x_{-q} - e^{-i2\pi Q} x_q) \quad (6a)$$

$$\ddot{x}_q = -\omega_q^2 x_q + \frac{\lambda}{2} e^{i2\pi Q} \quad (6b)$$

$$\ddot{x}_{-q} = -\omega_q^2 x_{-q} + \frac{\lambda}{2} e^{-i2\pi Q} \quad (6c)$$

In Fig. 2 we compare the behavior of $P(t) = \dot{Q}(t)$, obtained by solving the minimal set of Eqs. (6) with the appropriate initial conditions $Q(t=0) = 0$, $P(t=0) = P_0$,

$x_q(t=0) = \lambda/(2\omega_q^2)$, $\dot{x}_q(t=0) = 0$, with the one obtained from the full system of Eqs. (2). Eqs. (6) reproduce very well the initial behavior of the CM velocity which displays oscillations of frequency Δ around the value $\Omega/2\pi$. However, Eqs. (6) do not, of course, predict the decay occurring at later times because, as we show next, this is due to coupling to other modes. To this aim, we analyze the relation between the initial CM velocity P_0 and $\Omega/2\pi$, respectively Δ_{\pm} .

Take as an ansatz for the CM motion:

$$Q(t) = \frac{\Omega}{2\pi} t + \alpha_+ \sin(\Delta_+ t) + \alpha_- \sin(\Delta_- t) \quad (7)$$

If we insert the ansatz (7) in the coupled set of Eqs. (6) keeping only terms linear in α_{\pm} , we find that Δ_{\pm} are roots of one equation:

$$\Delta^2 = \lambda^2 \pi^2 (2Z(0) - Z(\Delta) - Z(-\Delta)) \quad (8)$$

$Z(\Delta)$ being the impedance

$$Z(\Delta) = \frac{1}{\omega_q^2 - (\Omega + \Delta)^2}. \quad (9)$$

In general Eq. (8) has (besides the trivial solution $\Delta = 0$) indeed two solutions, related to the sum and difference of the two basic frequencies in the system, ω_q and Ω :

$$\Delta_{\pm} \cong |\omega_q \pm \Omega + \frac{\lambda^2 \pi^2}{2\omega_q(\Omega \pm \omega_q)^2} + \dots| \quad (10)$$

Close to resonance, $\Omega \sim \omega_q$, the amplitude α_- dominates (see below) and the CM oscillates with a single frequency $\Delta = \Delta_-$ (see Fig. 2). Very close to resonance (more precisely $\omega_q < \Omega < \omega_q + (2\lambda^2 \pi^2 / \omega_q)^{\frac{1}{3}}$), the root Δ_- becomes imaginary, signaling an instability. In fact the system turns out to be bistable as it can be seen in Fig. 3 by the jump in $\Omega(P_0)$ as P_0 passes through $\omega_q/(2\pi)$.

Analytically, the relation between Ω and P_0 and the amplitudes α_{\pm} , is determined by matching the ansatz (7) with the initial condition:

$$\alpha_{\pm} = \frac{\lambda^2 \pi \Omega}{2\omega_q^2} \frac{1}{(\omega_q \pm \Omega)^3} \quad (11)$$

$$P_0 = \frac{\Omega}{2\pi} + \frac{\lambda^2 \pi \Omega}{2\omega_q^2} \left[\frac{1}{(\Omega + \omega_q)^2} + \frac{1}{(\Omega - \omega_q)^2} \right] + \dots \quad (12)$$

The fact that Eq. (12) has multiple solutions for Ω when $P_0 \sim \omega_q/2\pi$ is in accordance with the jump seen in Fig. 3. However, Eq. (12), which is derived by keeping only linear terms in α_{\pm} , is not accurate enough to describe in detail the instability in the above range around ω_q where α_- diverges.

An initial behavior similar to that for $P_0 \simeq \omega_q/2\pi$ is observed in Fig. 1 for $nP_0 \simeq \omega_{nq}/n2\pi$. We examine the case $n = 2$. Eq. (5) shows that x_{2q} is driven in next order in λ by x_q :

$$\ddot{x}_{2q} = -\omega_{2q}^2 x_{2q} + i2\lambda\pi e^{i2\pi Q} x_q \quad (13)$$

When $2\pi Q \simeq \Omega t$, x_q will be $\simeq \lambda e^{i\Omega t}$, so that x_{2q} is forced with amplitude λ^2 and frequency 2Ω , yielding resonance for $2\Omega = \omega_{2q}$. Since x_{2q} couples back to x_q , we have a set of equations similar to Eqs. (6), but at order λ^2 .

We now come to the key issue, namely the onset of friction causing the decay of the CM velocity seen in Fig. 1 at later times, which cannot be explained by the coupling of the CM to the main harmonics nq . Since x_q is by far the largest mode in the early stage, we consider second order terms involving x_q in Eq. (5):

$$\ddot{x}_k = -[\omega_k^2 + 2\lambda\pi^2 (e^{i2\pi Q} x_{-q} + e^{-i2\pi Q} x_q)] x_k \quad (14)$$

Insertion of the solution obtained above for x_q (Eq. (6b)) and Q (Eq. (7)) yields

$$\ddot{x}_k = -[\omega_k^2 + A + B \cos(\Delta t)] x_k \quad (15)$$

with $A = 2(\lambda\pi)^2/Z(0)$ and $B \sim \alpha_-$. Clearly, Eq. (15) is a Mathieu parametric resonance for mode x_k . The relevance of parametric resonances has been recently stressed in Ref. [11]. Note, however, that here, due to the coupling of the CM to the modulation mode q , resonances are not with the washboard frequency Ω but with $\Delta \sim \Omega - \omega_q$. Hence, we find instability windows around $\omega_k^2 + A = (n\Delta/2)^2$. Since Δ is small close to resonance, one expects to find instabilities for acoustic modes with k small. Indeed, as shown in Fig. 4a, we find by solving Eq. (2) that the decay of the CM is accompanied by the exponential increase of the modes $k = 2, 3, 4$ and, with a much longer rise time, $k = 1$. However, a closer look shows that the instability windows resulting from Eq. (15), shown in Fig. 4b, cannot explain the numerical results of Fig. 4a. This is due to the frequency shift A which moves the first Mathieu window to k values below $k = 1$, while the higher windows, which are higher order in B , are vanishingly small on the scale of the discreteness of the spectrum at $N = 144$. So the Mathieu formalism by itself cannot explain the observed instability. In Eq. (5), the only linear terms left out in Eq. (14) are couplings with $x_{k\pm q}$, which are much higher order in λ . Nevertheless, these terms turn out to be crucial since they may cause new instabilities due to the fact that, for k small, they are also close to resonance. We have solved the coupled set of equations for mode $x_{\pm k}$ and $x_{k\pm q}$:

$$\ddot{x}_k = -[\omega_k^2 + 2\lambda\pi^2 (e^{i2\pi Q} x_{-q} + e^{-i2\pi Q} x_q)] x_k + i\lambda\pi (e^{i2\pi Q} x_{k-q} - e^{-i2\pi Q} x_{k+q}) \quad (16a)$$

$$\ddot{x}_{k\pm q} = -[\omega_{k\pm q}^2 + 2\lambda\pi^2 (e^{i2\pi Q} x_{-q} + e^{-i2\pi Q} x_q)] x_{k\pm q} \pm i\lambda\pi e^{\pm i2\pi Q} x_k \quad (16b)$$

together with Eqs. (6) for continuous k . Indeed, we find a wider range of instabilities, giving a detailed account

of the numerical result as shown in Fig. 4b. This mechanism where a parametric resonance is enhanced by coupling to near resonant modes is quite general in systems with a quasi continuous spectrum of excitations and is related to the one proposed [15] in explaining instabilities in the FPU chain in a different physical context. It is noticeable that, even for this weak value of λ instabilities extend up to frequency $\omega \sim 0.2$, so that for this case, only systems with $N < 32$ are stable.

A full analytical analysis of these equations, based on the Floquet-Bloch ansatz, $x_k = e^{i\nu t} f(t)$ with f a function with period $2\pi/\Delta$, will be given elsewhere. Here we only want to point out that the matrix equation resulting from a cut-off in the Fourier series for f , has resonant poles in the off-diagonal terms. This explains the large width of the instability windows seen in the numerical analysis. The above described multiple parametric excitation gives rise to an effective damping for the system via a cascade of couplings to more and more modes via the non-linear terms in Eq. (5). It remains an open question whether this mechanism will eventually lead to a full or partial equilibrium distribution of dissipated energy over the normal modes [17] although our preliminary results support the former hypothesis even at very weak couplings.

In summary, we have described in detail the mechanism which gives rise to friction during the sliding of a harmonic system onto an incommensurate substrate. The onset of friction occurs in two steps: the resonant coupling of the CM to the modes with wavevector related to the substrate modulation leads to long wavelength oscillations which in turn drive a complex parametric resonance involving several resonant modes. This mechanism is robust in that it leads to wide instability windows and represents a quite general mechanism of energy transfer for systems with a quasi continuous spectrum of excitations.

We are grateful to Ted Janssen for many constructive discussions and for his support.

-
- [1] C. M. Mate, G. M. McClelland, R. Erlandsson, and S. Chiang, Phys. Rev. Lett. **59**, 1942 (1987).
 - [2] J. Krim, D. H. Solina, and R. Chiarello, Phys. Rev. Lett. **66**, 181 (1991). J. B. Sokoloff, J. Krim, and A. Widom, Phys. Rev. B **48**, 9134 (1993).
 - [3] *Physics of Sliding Friction*, edited by B. N.J. Persson and E. Tosatti (Kluwer, Dordrecht, 1996); B. N. J. Persson, Surf. Sci. Rep. **33**, 83 (1999).
 - [4] K. Shinjo and M. Hirano, Surf. Sci. **283**, 473 (1993).
 - [5] S. Aubry and L. de Seze, Festkörperprobleme **XXV**, 59 (1985).
 - [6] O. M. Braun, T. Dauxois, M. V. Paliy, and M. Peyrard, Phys. Rev. Lett. **78**, 1295 (1997); Phys. Rev. E **55**, 3598 (1997).
 - [7] T. Strunz and F.-J. Elmer, Phys. Rev. E **58**, 1601 (1998); **58**, 1612 (1998).
 - [8] Z. Zheng, B. Hu, and G. Hu, Phys. Rev. B **58**, 5453 (1998).
 - [9] J. B. Sokoloff, Phys. Rev. Lett. **71**, 3450 (1993); J. Phys. Cond. Matt. **10**, 9991 (1998).
 - [10] Y. Braiman, F. Family, and H. G. E. Hentschel, Phys. Rev. B **55**, 5491 (1997).
 - [11] H. G. E. Hentschel, F. Family, and Y. Braiman, Phys. Rev. Lett. **83**, 104 (1999).
 - [12] Ya. I. Frenkel and T.A. Kontorova, Zh. Eksp. Teor. Fiz. **8**, 89 (1938).
 - [13] S. Aubry and G. André, in *Annals of the Israel Physical Society*, **3**, edited by L. P. Horowitz, Y. Ne'eman and Adam Hilger (Bristol, 1980), p. 133.
 - [14] *Handbook of mathematical functions*, edited by M. Abramowitz and I. A. Stegun (Dover, New York, 1970).
 - [15] G. Christie and B. I. Henry, Phys. Rev. E **58**, 3045 (1998).
 - [16] See, e.g., Eq. (3) in T.S. van Erp, A. Fasolino, O. Radulescu, and T. Janssen, Phys. Rev. B **60**, 6522 (1999).
 - [17] J. De Luca, A. J. Lichtenberg, and S. Ruffo, Phys. Rev. E **60**, 3781 (1999).

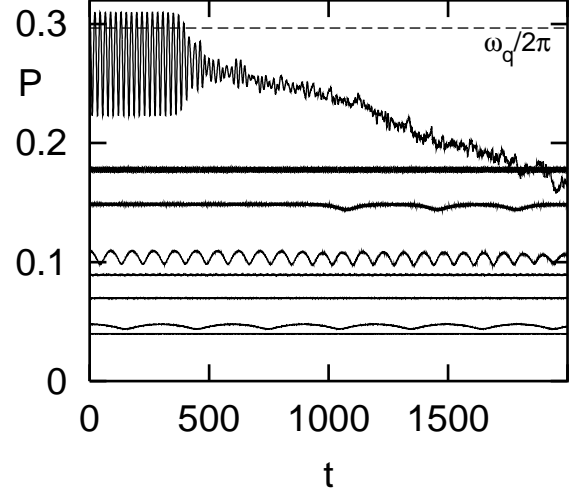


FIG. 1. Time dependence of the CM velocity for several values of P_0 for $N = 144$, $\lambda = 0.015 \sim \frac{\lambda_c}{3}$. The dashed line corresponds to $P_0 = \frac{\omega_q}{2\pi} = 0.2966$. Analogous behavior occurs at velocities near $\frac{1}{2} \frac{\omega_{2q}}{2\pi} = 0.1075$ and $\frac{1}{3} \frac{\omega_{3q}}{2\pi} = 0.0469$.

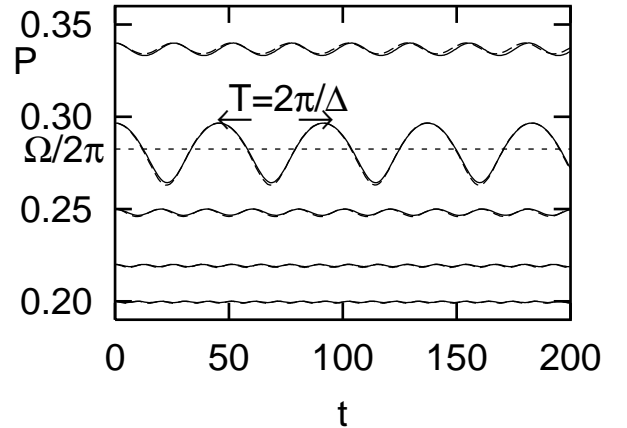


FIG. 2. Comparison between the simulation of the FK system according to Eq. (2) (solid lines) and the numerical solution of Eqs. (6) for $N = 144$, $\lambda = 0.015$, and several values of P_0 (dashed lines). The horizontal dashed line indicates $\Omega/2\pi$ for $P_0 = 0.29$.

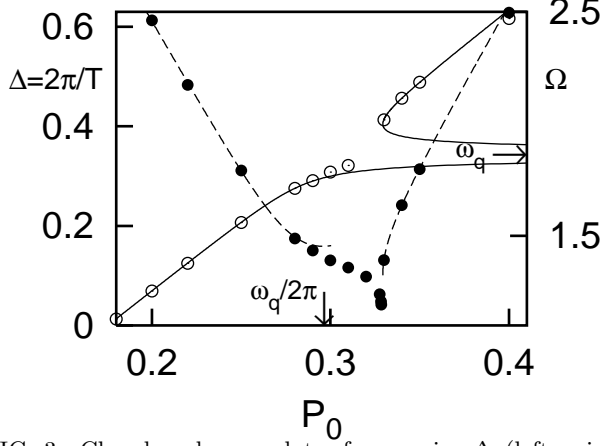


FIG. 3. Closed and open dots, frequencies Δ (left axis) and Ω (right axis) versus P_0 for simulations for $N = 144$, $\lambda = 0.015$. Dashed and solid lines: solutions of Eqs. (10) and (12) respectively.

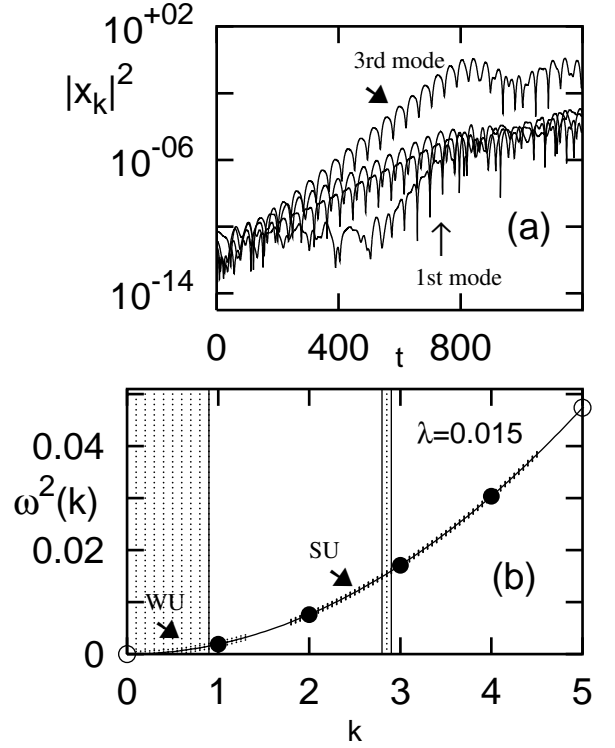


FIG. 4. (a) $|x_k(t)|^2$ of the first 4 modes from Eq. (2) with $N = 144$, $\lambda = 0.015$ and $P_0 = 0.29$. Note that the first mode has a longer rise time and that the third mode is the most unstable. (b) Dispersion relation for a chain of 144 atoms (k -values in units of $(\frac{2\pi}{144})$). Unstable modes resulting from the full simulation are represented by solid dots. The shaded k -ranges give the instability windows resulting from the Mathieu-type Eq.(14) and cannot explain the simulation. Conversely the wiggled ranges of the phonon dispersion (WU=weakly unstable, SU=strongly unstable) are the instability windows predicted by Eqs. (6) and (17). They explain all instabilities as well as the long rise time of the first mode (WU) and the shortest one of the third mode which falls in the middle of the SU range.

